LA-UR-21-22876
Approved for public release; distribution is unlimited.

Title: Evaluation of relationship between post-injection plume stability and leakage risks

Author(s): Pawar, Rajesh J.
Chu, Shaoping
Makedonska, Nataliia
Onishi, Tsubasa
Harp, Dylan Robert

Intended for: 15th International Conference on Greenhouse Gas Control Technologies, GHGT-15, 2021-03-15 (Abu Dhabi, United Arab Emirates)

Issued: 2021-03-24

15th International Conference on Greenhouse Gas Control Technologies, GHGT-15

15th 18th March 2021 Abu Dhabi, UAE

Evaluation of relationship between post-injection plume stability and leakage risks

Rajesh Pawar [a]*, Shaoping Chu[a], Nataliia Makedonska[a], Tsubasa Onishi[b], Dylan Harp[a]

[a]*Earth & Environmental Sciences Division, Los Alamos National Laboratory, Los Alamos, NM, USA, 87545*
[b]*Department of Petroleum Engineering, Texas A&M University, College Station, TX, USA, 77843*

Abstract

One of the critical questions for geologic CO_2 storage is how long should a storage site be monitored after the injection is stopped. A storage site operator is required to demonstrate that the storage site is evolving towards long-term stability and the injected CO2 as well as reservoir pressure do not pose any threat including to the groundwater. Migration and evolution of injected CO_2 plume depend on site-specific geologic structure, storage reservoir properties as well as operational conditions. While injected CO_2 plume may continue to evolve after injection is stopped, its dynamic evolution does not directly imply imminent leakage risk. Leakage risks depend on multiple factors including not only CO_2 presence but also reservoir pressure and the characteristics of potential leakage pathways. We performed a modeling based study to evaluate the relationship between post-injection plume migration and leakage risks. Our hypothetical case study is based on the Rock Springs Uplift in southwestern Wyoming in USA. We used a numerical model to perform multiple sets of reservoir simulations each with 29 equi-probable realizations of reservoir permeability heterogeneity, simulating different injection scenarios. We applied newly developed moment-based plume mobility metrics to characterize the migration and evolution of injected CO_2 plume. The plume mobility metrics provided detailed analyses of the effect of reservoir permeability heterogeneity and CO_2 injection rate on spatial and dynamic evolution of CO_2 and overpressure plume. Next, we assessed the potential leakage risks using the integrated assessment modelling approach developed by US DOE's National Risk Assessment Partnership (NRAP). The combined leakage risk assessment and plume mobility analyses results indicate that lack of CO_2 plume stability (or non-zero plume mobility) may not directly imply groundwater aquifer endangerment and the leakage risks are dependent on multiple factors, including presence of wells and their locations and types.

This paper is a condensed version of a peer-reviewed paper by Pawar et al [1] published in the International Journal of Greenhouse Gas Control.

Keywords: : PISC; Plume Stability; Post-injection leakage risks

1. Introduction

The US-EPA regulations for Class VI wells for geologic CO_2 storage (GCS) require a site to be monitored after the

* Corresponding author. Tel.: +1-505-665-6929, *E-mail address:* rajesh@lanl.gov

injection is stopped until it can be successfully demonstrated that the underground sources of drinking water (USDW) within the vicinity are no longer under threat from injected CO_2 or in-situ pressures. While the default post-injection site care (PISC) period is 50 years, a GCS site operator can request an alternate time frame if non-endangerment of groundwater can be successfully demonstrated [2]. This requires utilizing the monitoring observations coupled with predicted rates of CO_2 plume migration and predicted time frame for the cessation of migration [3]. Multiple modelling studies and a few field tests demonstrate that evolution of CO_2 plume and pressure front at a GCS site are strongly influenced by site-specific geologic complexity and operational conditions during the injection phase as well as after the injection is stopped [4, 5, 6, 7, 8, 9, 10]. The magnitude of overpressure in the reservoir, overpressure area, maximum pressure and the rates at which the pressure increases (during injection) and decreases (after injection is stopped) depend on the geologic structure, heterogeneity in permeability, sand continuity, in-situ hydrologic conditions, fluid properties, injection rate and injection duration. Similar to pressure, the site-specific parameters and operational conditions mentioned above as well as topography affect the spatial extent of free-phase CO_2 plume and its migration during the injection and post-injection phases. Site-specific geologic complexity can lead to complex CO_2 plume evolution [11]. Effective characterization of CO_2 and pressure plume require metrics that can effectively capture its important characteristics, such as the location of the centroid of plume mass, the primary direction in which the plume spreads, the amount of spreading in the primary and secondary directions [12]. These metrics provide information that can be used to assess whether evolution and migration of CO_2 plume can potentially lead to endangerment of groundwater. Endangerment of groundwater from CO_2 during the post-injection phase ultimately depends on whether the mobile, free-phase CO_2 encounters a leakage pathway and if the combination of reservoir pressure and buoyancy of CO_2 is sufficient to push it through the leakage pathway into the USDW. A systematic risk assessment can help to quantify the groundwater endangerment risks and determine monitoring requirements to manage and mitigate them. US-DOE's National Risk Assessment Partnership (NRAP) has developed an Integrated Assessment Modeling (IAM) approach for quantifying environmental risks due to leakage at GCS sites [13]. The IAM approach takes into consideration dynamic evolution of CO_2 saturation and pressure in the storage reservoirs over the lifetime of a GCS site and predicts potential migration of CO_2 and brine into groundwater aquifer through different leakage pathways and resulting impacts. This study is focused on assessing whether demonstration of plume stability is necessary to demonstrate non-endangerment of groundwater. We use a modeling based approach that includes numerical simulations of CO_2 injection at a geologically complex storage site, computation of various metrics that characterize evolution of CO_2 plume and pressure front in the reservoir during and after CO_2 injection, quantification of risk to groundwater due to leakage and assessment of correlation between migration of CO_2 plume and leakage risks.

2. Reservoir Simulation of CO_2 Injection and Post-injection Behavior

We use a numerical reservoir model based on the Rock Springs Uplift (RSU), a doubly dipping anticline, in southwestern Wyoming [14]. The primary storage reservoirs at RSU include the Weber sandstone and Madison limestone with structural trapping provided by the overlying Phosphoria and Chugwater formations, all of which dip at 4°, primarily in the southwest to northeast direction. A geologic model for the site has been developed using site-specific geologic data, including wellbore density logs and neutron porosity logs. The main geological formations are further subdivided into high, medium and low permeability sub-regions based on the permeability values derived from combined core and log analyses. To provide uncertainty bounds on reservoir pressure and saturation changes we developed 29 equally-likely realizations of heterogeneous permeability using a geostatiscial approach described by Deng et al [15].

We simulated multiple scenarios of CO_2 injection by varying the injection rate (0.1, 1, 5 Mt/yr), injection duration (3, 10 years), post-injection duration (upto 90 years) and boundary conditions (closed and open). We assume that the injection rate constraint is honoured irrespective of injection pressure (i.e. no maximum injection pressure limit). We used two different model domain sizes, namely 16 km x 16 km and 100 km x 100 km. We performed 29 reservoir simulation runs (using 29 permeability realizations) for each injection scenario and each model domain. To get additional details about the scenarios and numerical model setup as well as all the results related to this work the reader is referred to Pawar et al [1]. Here we discuss some of the results for the smaller model (16 km x 16 km).

2.1. Plume mobility metrics

The results discussed here are for the injection scenario with 1 MT/yr injection for 10 years followed by a 90 year post-injection period and open lateral boundaries (fixed pressure boundary condition). We computed various plume metrics developed by Harp et al [12] to characterize the reservoir pressure and CO_2 saturation plumes using the simulation results for each of the 29 permeability realizations. The computed plume metrics included 1) area of reservoir over which the overpressure exceeded a critical overpressure value (overpressure plume area), 2) area of reservoir over which the CO_2 saturation was non-zero (CO_2 plume), 3) the rate of change of overpressure plume area, 4) the rate of change of CO_2 plume area, 5) the location of centroid of CO_2 plume in the reservoir, 6) the velocity (x & y components) of the centroid of CO_2 plume, 7) the primary and secondary directions of CO_2 plume spreading, 8) the rate of spreading of CO_2 plume in the primary and secondary directions. To compute the metrics related to overpressure plume we first estimated the critical overpressure value using site-specific parameters and one of the approaches suggested by US-EPA [16]. The EPA recommended approach defines critical overpressure as the magnitude of pressure increase needed to lift the in-situ brine through a hypothetical open borehole into an overlying USDW. For our study area the critical overpressure was estimated to be 1.18 MPa. Fig. 1 shows the plots of time-dependent areas of overpressure and CO_2 plumes. The plots show mean values computed from the 29 simulation runs corresponding to 29 permeability realizations.

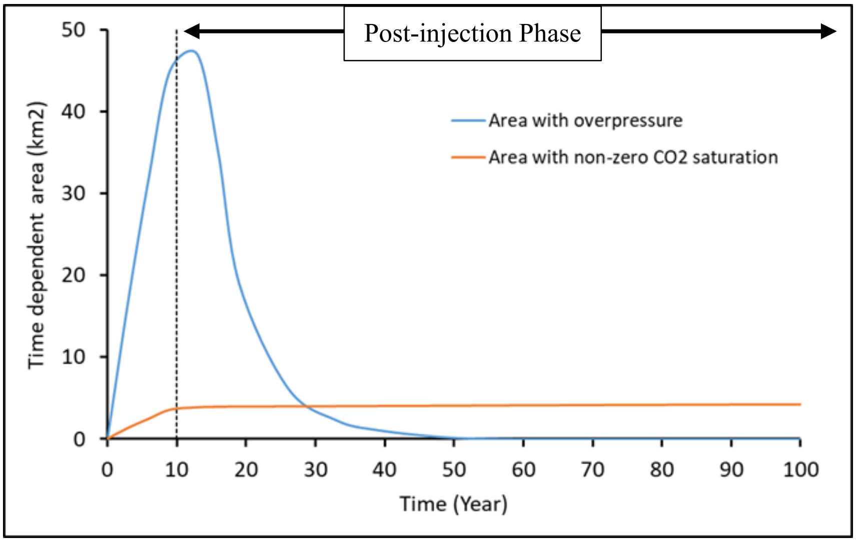

Fig.1. Time-dependent areas of overpressure and CO_2 plume in the storage reservoir.

The size of the area of overpressure is significantly larger than that of CO_2 plume. It takes some time after the injection is stopped before the pressure in the reservoir starts to relax and the area of overpressure starts to decrease. Unlike the area of overpressure, the area for CO_2 plume reaches a maximum and remains nearly constant. A constant CO_2 plume area does not necessarily imply that injected CO_2 plume stops moving but as will be discussed later it continues to migrate and evolve. We have not simulated dissolution of CO_2 in in-situ brine and reaction of CO_2-dissolved brine with reservoir rocks. If these processes were taken into account the CO_2 plume area will also decrease with time. It is widely expected in the GCS research community that there will be difference in the areas of overpressure and CO_2 plume in most storage reservoirs. The magnitude of difference between the two as well as which of the two will be higher will depend on the site-specific geologic parameters and site operational conditions. This overall concept of different overpressure and CO_2 plume areas has been used to propose a tiered Area of Review (AoR) approach by Birkholzer et al [17]. The tiered AoR approach can reduce the cost of pre-injection site characterization as well as monitoring during and after injection.

Fig. 2 shows the trend in migration of CO_2 plume over time using the locations of CO_2 plume centroid over 100 years. The centroid locations at different times including, after 1 year of injection, 9 years of injection (one year before

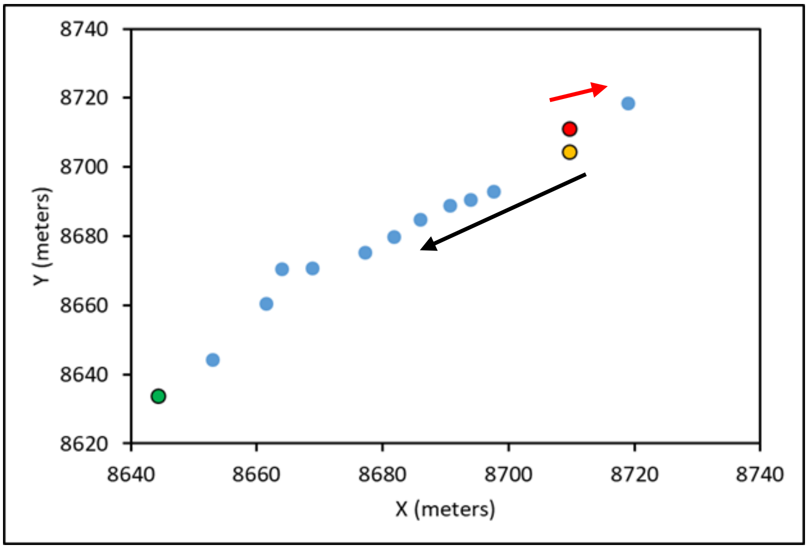

Fig.2. CO_2 plume centroid locations over time. Red circle corresponds to centroid location after 1 year, yellow circle corresponds to centroid location after 9 years while the green circle corresponds to centroid location after 0 years. The red arrow indicates centroid movement during early time while the black arrow indicates movement during later time including post-injection period.

injection stops) and 90 years after the injection is stopped are highlighted in the figure. The plume centroid locations demonstrate the effect of 4º reservoir dip (in SW-NE direction) on evolution of injected CO_2 plume. During injection phase the migration of plume centroid is a result of the combined effect of reservoir geologic complexity and pressure drive imposed by injection while during the post-injection phase the pressure drive is reduced as pressure relaxes and free-phase CO_2 migration is mainly controlled by the reservoir geology and buoyancy of mobile CO_2. In addition to the locations of plume centroid we also compute velocity of plume centroid to get an estimate of plume migration. The x and y directional components of CO_2 plume centroid velocity over time are plotted on Fig. 3.

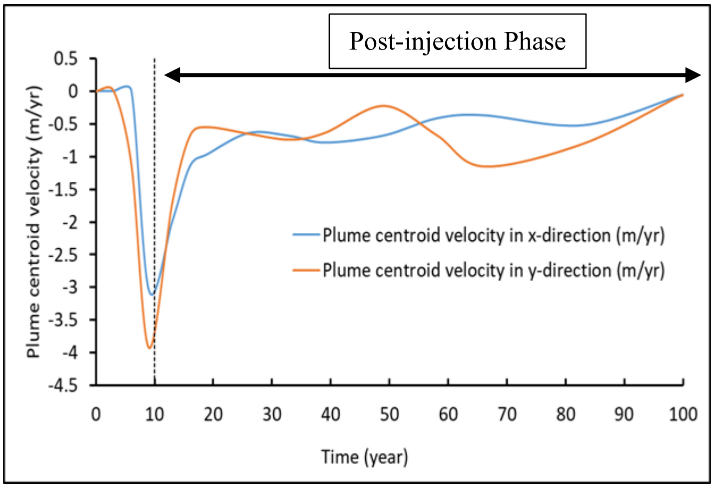

Fig.3. The mean directional velocity of CO_2 plume centroid over time computed from 29 simulation runs.

The maximum magnitude of plume centroid velocity reaches 4 meters/year and decreases to < 1 meter/yr before reducing to zero during post-injection phase. At this rate the plume centroid (hence, majority of injected CO_2) is not expected to migrate a significant distance. The effect of reservoir slope on CO_2 migration can be seen through dynamic velocity trends. The velocities are negative [movement is occurring in the negative x (west) and y (south) directions] through the combined injection and post-injection phases. The magnitude of velocity increases through the injection phase and reaches a maximum at the end of injection demonstrating influence of injection pressure and the reservoir dip. The non-zero centroid velocity during post-injection phase demonstrates CO_2 plume movement under the influence of reservoir dip (through buoyancy) while the variations in velocity magnitude as well as the relative velocity magnitudes in the x and y directions demonstrate the influence of permeability heterogeneity on CO_2 plume migration. The risk assessment process needs to take into consideration not only migration of CO_2 plume but also how the plume occupies areal space in the reservoir. The shape of injected CO_2 plume and its spreading can be complex depending on reservoir geologic complexity. To characterize the evolution of CO_2 plume shape we compute two metrics, the primary and secondary directions in which the plume spreads and the rate of plume spreading in the primary and secondary directions. Fig. 4 shows the plots of time-dependent variation in the mean primary and secondary directions in which the CO_2 plume spreads. During injection phase the CO_2 plume grows in a complex manner where the primary and secondary directions in which the plume spreads vary with time but during the post-injection phase the primary spreading occurs in the general direction of the reservoir dip.

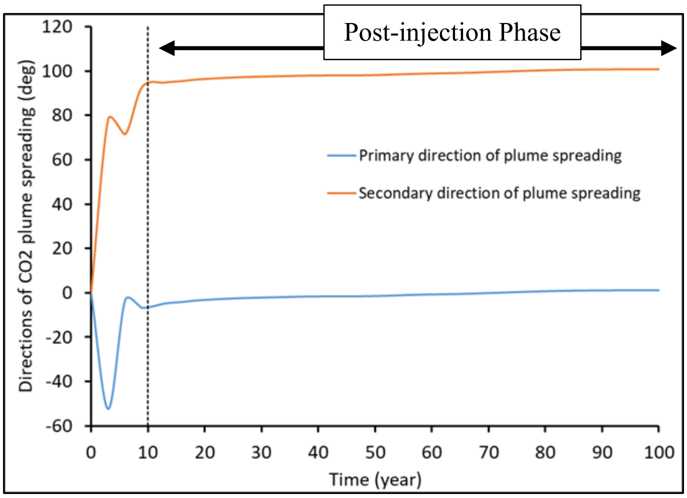

Fig. 4. Time-dependent variation in the primary and secondary directions of plume spreading. Plots show mean values computed from 29 simulation runs. Zero degree direction coincides with +ve x direction.

The rate of plume spreading is computed as the time derivative of the plume spreading metric and is plotted on Fig. 5. The rate increases with time until it reaches a maximum value which happens before the injection is stopped (unlike the plume area shown in Fig. 1). The decrease in CO_2 plume spreading rate does not mean that plume is not spreading as more CO_2 is being introduced. As more CO_2 is being introduced in the system it occupies more reservoir pore volume but the rate at which newly injected CO_2 occupies pore volume eventually reaches a plateau and starts to decrease as the occupied volume increases. The time at which this happens is dependent on site-specific geologic conditions (porosity, thickness and permeability). The overall trend of decreasing rate of CO_2 plume spreading with time is also observed in plume centroid velocity and rate of change in the plume area over time. This is an important observation for predicting long-term plume evolution as well as migration behaviour with implications on duration of post-injection monitoring deployment. If the monitoring observations consistently indicate that plume area is constant while plume centroid velocity and plume spreading rate are decreasing, the long-term trend will imply that the plume may be becoming less mobile. The observed time dependent behaviour can then be used to project CO_2 plume movement up to where metrics such as plume centroid velocity and plume spreading rate will reach zero (or become negative) and these estimates can subsequently be used to determine the post injection site care duration.

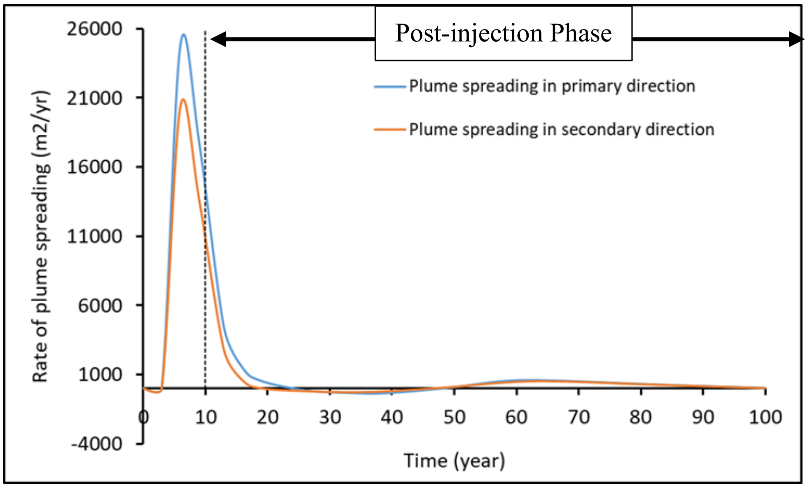

Fig. 5. Time-dependent variation in the rates of plume spreading in the primary and secondary directions. Plots show mean values computed from 29 simulation runs.

2.2. *Influence of geologic heterogeneity and operational parameters*

The effect of permeability heterogeneity and uncertainty is demonstrated by plotting the mean, maximum and minimum values computed over 29 realizations on Fig. 6 (overpressure area) and Fig. 7 (CO_2 plume area). While the figures show variability in plume areas across the ensemble, the general trend in each plume's time-dependent behaviour remains across the ensemble. Fig. 6 shows that the uncertainty in permeability can affect both the maximum overpressure area (which has implications on AoR estimates) as well as predicted time at which the reservoir pressure falls below the critical overpressure threshold (which has implications of PISC duration). Similarly, Fig. 7 shows the variability in the maximum CO_2 plume area and the time at which the plume area reaches the maximum value. Overall, all the CO_2 plume areas show similar time-dependent trend over 29 permeability realization.

As mentioned earlier, we simulated multiple injection scenarios by varying injection rate and injection duration and for each injection scenario we performed 29 different simulation runs sampling the 29 permeability distributions. The ensemble mean of the plume metrics computed from the simulation results were used to assess the influence of injection conditions. Figures 8 & 9 show the effect of injection rate on the overpressure area, CO_2 plume area and their respective time derivatives. While the overall trends in the plume areas and their derivative remain the same, their magnitudes are directly affected by injection rate. The size of both plume areas and the magnitude of time derivatives increase with the injection rate. It takes longer for the time derivative to reach zero for higher injection rates particularly, for the derivative of CO_2 plume area. The non-zero overpressure area at 100 years for the highest injection rate (5 MT/yr) implies that it takes longer than 100 years for the overpressure to go to zero.

Above results demonstrate the complexities in the dynamic evolution of CO_2 and overpressure plumes and the impact of geologic complexity as well as operational conditions on their evolution.

3. Integrated Assessment Modeling for Leakage Risk Assessment

In order to understand potential relationship between injected CO_2 and overpressure plumes and leakage risks to groundwater aquifer, we applied NRAP's Integrated Assessment Model (NRAP-IAM-CS, 13) to the RSU site to perform hypothetical leakage simulations. The site-specific IAM model included a storage reservoir, a (hypothetical) legacy well and a shallow groundwater aquifer. It is important to note that there are no legacy wells within the RSU domain considered in our study and its use in our model is solely for demonstration. For shallow groundwater aquifer we used the properties of the Rocksprings aquifer [18]. In order to assess the effect of spatial evolution of reservoir pressure and CO_2 saturation on leakage risks, we simulated multiple scenarios by varying locations (Fig. 10) and integrity of the hypothetical legacy.

To assess the effect of wellbore integrity we simulated three different well type scenarios, namely, an open well

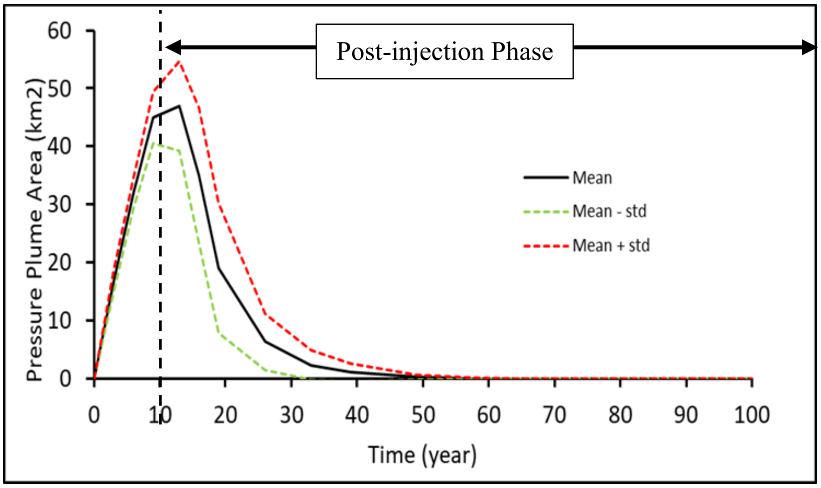

Fig. 6. Variability in overpressure area for ensemble simulations with 29 permeability realizations.

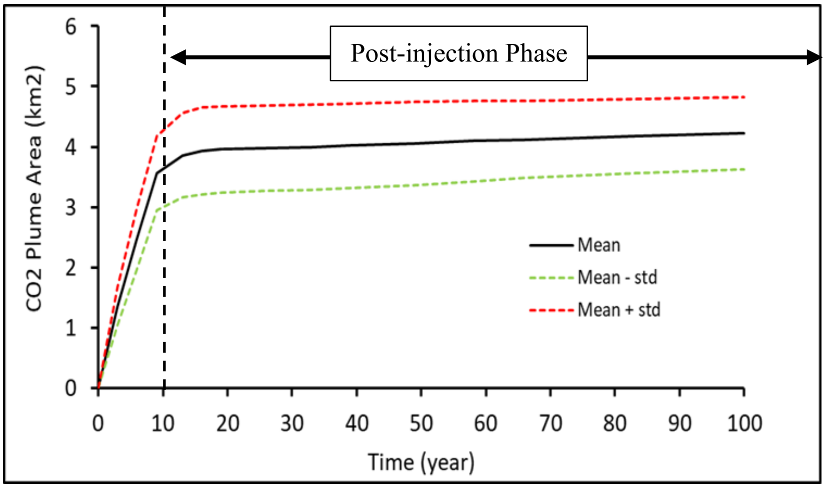

Fig. 7. Variability in CO_2 plume area for ensemble simulations with 29 permeability realizations.

(worst possible leakage scenario), cemented well with 50 Darcy cement permeability and cemented well with 1 Darcy cement permeability. Note that, all of the cases we simulated represent scenarios with wells with poor integrity (damaged cement). Overall we simulated 18 different scenarios through combinations of legacy well locations (6 locations) and well types (3 types) for each of the injection scenarios mentioned earlier. NRAP-IAM-CS uses reduced order models to simulate CO_2 migration through different components of the integrated model and its impact. For the storage reservoir, a look-up table approach is used where results of numerical simulations of CO_2 injection as well as post-injection are used to generate look-up tables containing time-dependent values of CO_2 saturation and pressure in the storage reservoir. These values are subsequently used during the IAM simulation run to compute leakage through a legacy well by an internal reduced-order-model for wellbore leakage. For each injection scenario we performed a NRAP-IAM-CS Monte-Carlo simulation utilizing results of 29 different reservoir simulation runs. Each of the IAM run simulated GCS site performance over 100 years which included a 10 years injection phase followed by a 90 years post-injection phase. The IAM simulation results included predicted leak rates of CO_2 and brine into a groundwater aquifer and the impact of CO_2 and brine leakage on the groundwater aquifer in terms of changes in pH and

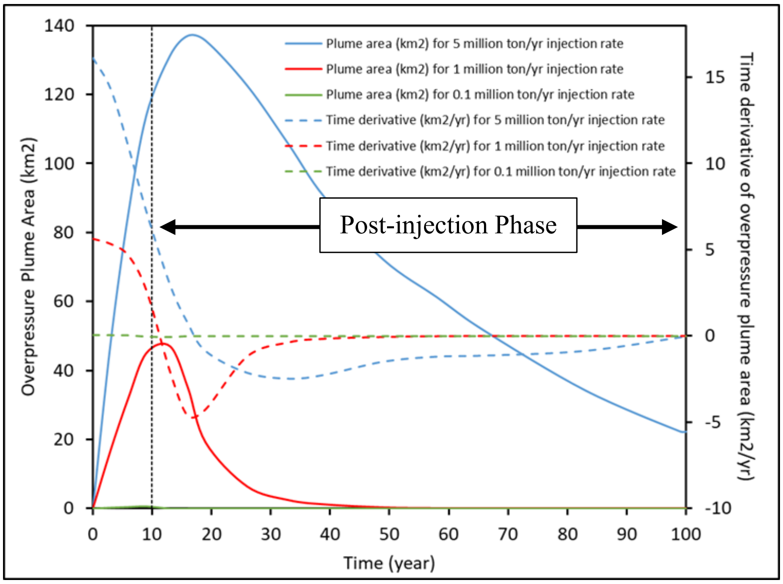

Fig. 8. The overpressure area and its time-derivative for 3 different injection rates at same total injection duration.

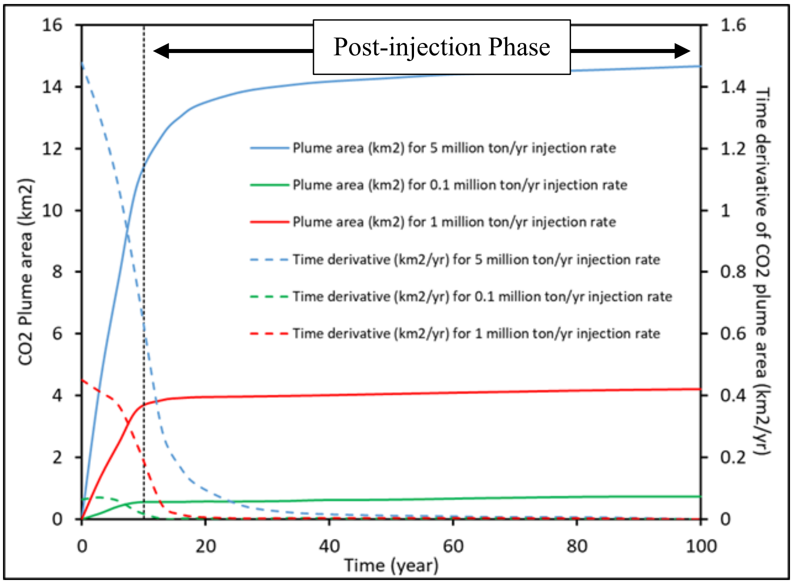

Fig. 9. The CO_2 plume area and its time-derivative for 3 different injection rates at same total injection duration.

concentration of total dissolved solids (TDS). NRAP-IAM-CS model computes the pH impact as the volume of groundwater where pH drops below 6.6 and TDS impact as the volume where TDS increases above 1300 ppm. Given that our interest is to assess risks to groundwater aquifer, we only discuss the potential for impacts of CO_2 and/or brine leakage into it. The plot on Fig. 11 shows potential of pH impact noted by the occurrence or absence of impact using a bar chart, where a bar with non-zero height notes impact and lack of height notes no-impact. The bars are plotted as a function of distance of the (hypothetical) legacy well from the injection, well types (open well, cemented well with

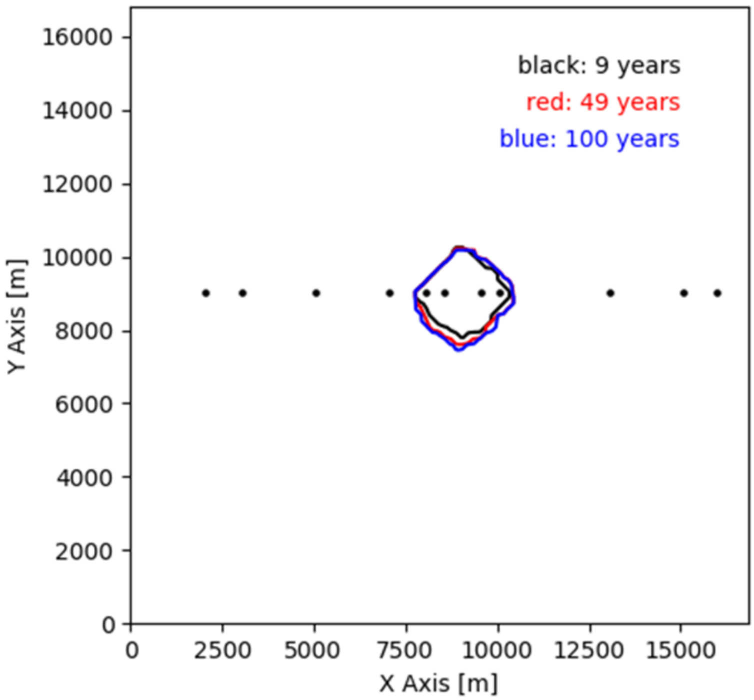

Fig. 10. A schematic diagram showing hypothetical well locations used for leakage risk assessment (the contours show the boundaries of injected CO_2 plume at different times for an example injection simulation run and the black dots represent hypothetical well locations).

50 Darcy cement permeability and cemented well with 1 Darcy cement permeability) and injection rates (0.1 Mt/yr, 1 Mt/yr & 5 Mt/yr).

Fig. 11 shows that a pH impact on the groundwater is only possible if there is an open wellbore within 2 km of the injector. For wells with cement as high 50 Darcy permeability there is no pH impact. Similar to the pH impact on Fig.11, the potential for TDS impact due to leakage is plotted using a bar chart on Fig. 12. Unlike the pH impact results, leakage from cemented wellbore with 50 Darcy permeability results in TDS impact for the two higher injection rates (1 & 5 million tons/yr) but the potential for impact exists if the well is located within 500 meters from the injection well for injection rate 1 Mt/yr and 2 km for injection rate 5Mt/yr. On the other hand, leakage through an open well located anywhere within the reservoir leads to TDS impact for the two higher injection rates.

Fig. 13 shows the time at which pH impact due to CO_2 leakage is observed in groundwater aquifer. The results demonstrate that the timing is affected by injection rate, wellbore type as well as wellbore location. For our site specific parameters wells with a cement permeability of 50 Darcy or below do not result in any pH impact. For the open well, the time of impact changes with injection rate and varies inversely with rate.

The results above show that leakage risks are non-existent for wellbores with cement permeability below 1 Darcy and mostly non-existent for wellbores with cement permeability of 50 Darcy except for high injection rates. The reported values of cement permeability based on a few field measurements to date are between 0.01 to 5 mili Darcy [19, 20, 21], which are well below the lowest permeability used in our study. Given that the CO_2 and brine leak rates are inversely proportional to wellbore cement permeability, the leak rates and resulting impacts to groundwater aquifers for permeability lower than 1 Darcy will be much lower than the ones reported in our study or even non-existent.

4. Summary

Our study results demonstrate that the geologic complexity at a GCS site and site operational parameters affect the

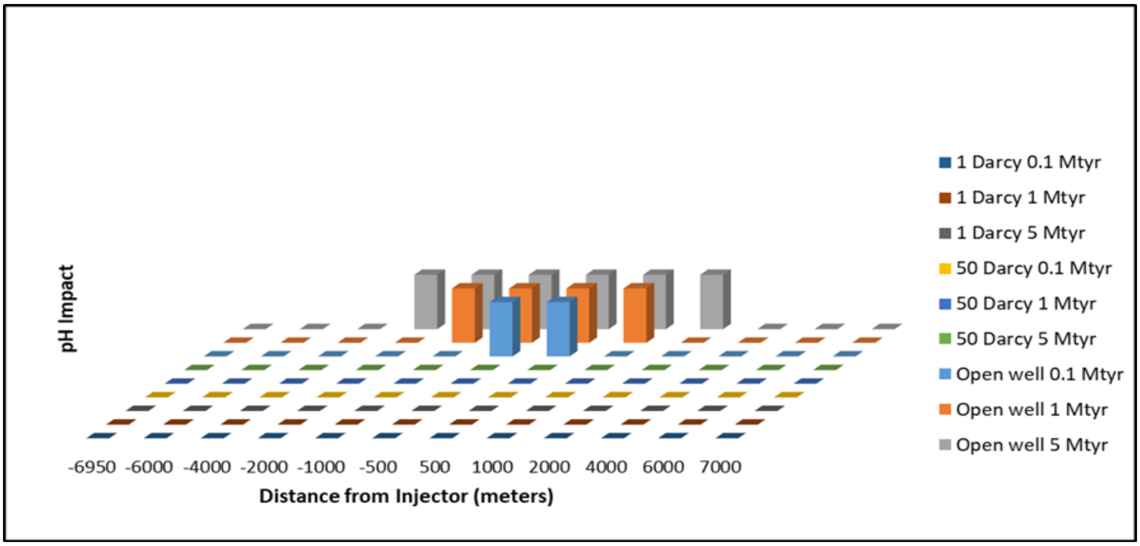

Fig. 11. Plot showing pH impact due to CO_2 leakage into groundwater aquifer from wells of 3 well types as a function of distance of the well from the injector. The plot shows results for 3 different CO_2 injection rates.

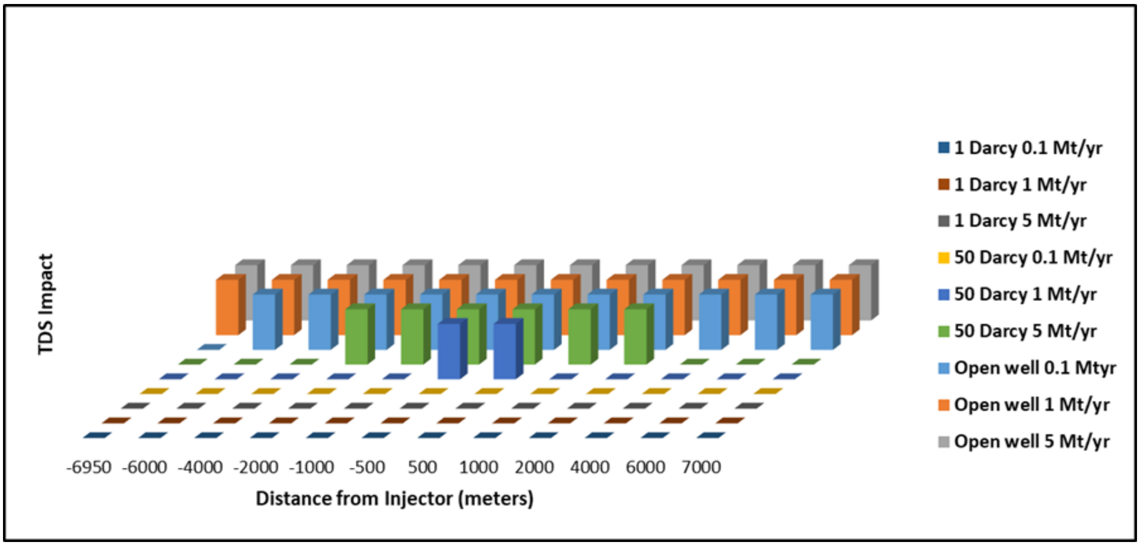

Fig. 12. Plot showing TDS impact due to CO_2 leakage into groundwater aquifer from wells of 3 well types as a function of distance of the well from the injector. The plot shows results for 3 different CO_2 injection rates.

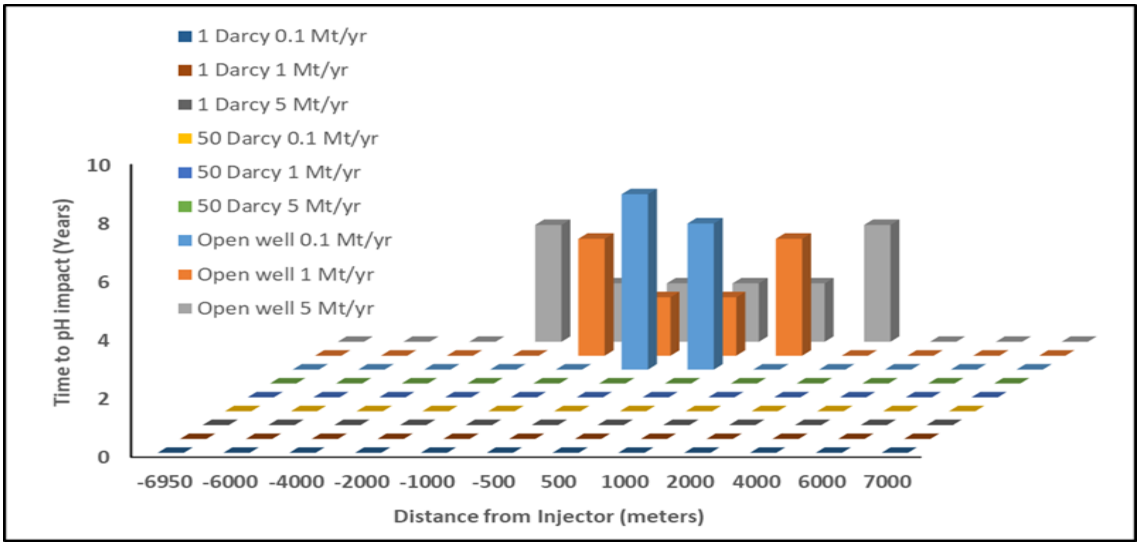

Fig. 13. Plot showing the time to pH impact due to CO_2 leakage into groundwater aquifer from wells of 3 well types as a function of distance of the well from the injector.

evolution and migration of injected CO_2 and reservoir pressure. The plume areas for critical overpressure (change in reservoir pressure over initial reservoir pressure exceeding critical pressure) and CO_2 plume can differ significantly and the magnitude of difference will depend on the geologic complexity as well as injection rate. The time dependent behaviour and difference in the overpressure and CO_2 plume areas can be used to support time-dependent AoRs. The characteristics of time-dependent behaviour of these plume areas and different plume metrics can be used to determine post-injection monitoring strategy.

Our leakage risk assessment demonstrates that the leakage risks are primarily affected by wellbore type and locations. The metrics used to quantify dynamic CO_2 plume evolution show that the plume continues to evolve during the post-injection phase but in spite of plume evolution the risk to the groundwater aquifer due to CO_2 leakage in the form of pH impact is non-existent and exists only for an extremely conservative scenario of an open wellbore located in an area smaller than the CO_2 plume area. Similarly, the overpressure in the reservoir remains above critical overpressure for a considerable time during post-injection phase but leakage risk quantification results show that the risks to a groundwater aquifer due to leakage of CO_2 and brine in the form of TDS impact is present for an extremely conservative scenario of an open wellbore and are virtually non-existent for cemented wellbores except for cement permeability of 50 Darcy but over a limited distance away from the injector. Both of these results effectively demonstrate that in spite of evolution of reservoir pressure and CO_2 saturation in the storage reservoir during the post-injection phase, the risks to groundwater aquifer due to leakage primarily depend on locations and type of wells present at the site. Our results also demonstrate that continued evolution of reservoir conditions during the post-injection phase does not necessarily imply endangerment of groundwater aquifer. Risk assessment coupled with numerical predictions can facilitate demonstration of non-endangerment in spite of lack of stability of injected CO_2 plume and continued evolution of reservoir pressure which in turn can help justify alternate post-injection monitoring time period compared to the default post-injection site care timeframe.

Acknowledgements

This work was supported by the US Department of Energy through the Los Alamos National Laboratory. Los Alamos National Laboratory is operated by Triad National Security, LLC, for the National Nuclear Security Administration of U.S. Department of Energy (Contract No. 89233218CNA000001). This work was completed as part of the National Risk Assessment Partnership (NRAP) project. Support for this project came from the U.S. Department of Energy's (DOE) Office of Fossil Energy's Coal Research program. The authors wish to acknowledge

Mark McCoy and Mary K. Underwood (NETL Strategic Center for Coal) and Mark Ackiewicz and Darin Damiani (DOE Office of Fossil Energy) for programmatic guidance, direction, and support.

References

[1] Pawar, RJ, Chu, SP, Makedonska, N, Onishi, T, Harp, D. Assessment of relationship between post-injection plume migration and leakage risks at geologic CO2 storage sites. Int. J. Greenh. Gas Control. 2020;101:103138.
[2] EPA, 2010. Federal Requirements Under the Underground Injection Control (UIC) Program for Carbon Dioxide (CO2) Geologic Sequestration (GS) Wells, in: Regulations, U.S.C.o.F. (Ed.), 40 CFR 146.81 et seq., 75 FR 77230. USEPA, Washington, DC.
[3] EPA, 2018. Geologic sequestration of carbon dioxide – Underground Injection Control (UIC) program class VI implementation manual for UIC program directors. Washington, DC.
[4] Hovorka, SD, Sakurai, S, Kharaka, YK, Nance, HS, Doughty, C, Benson, SM, Freifeld, BM, Trautz, RC, Phelps, T, Daley, TM. Monitoring CO_2 storage in brine formations: lessons learned from the Frio field test one year post injection. Proceedings of the 2006 UIC Conference of the Groundwater Protection Council, Abstract 10. GCCC Digitial Publication Series #06-06 2006.
[5] Goater AL, Bijeljic B, Blunt MJ. Dipping open aquifers – The effect of top-surface topography and heterogeneity on CO_2 storage efficiency. Int. J. Greenh. Gas Control 2013;17:318-31.
[6] Mishra, S, Oruganti, Y, Gupta, N, Ganesh, PR, McNeil, C. Modeling CO_2 plume migration based on calibration of injection and post-injection pressure response at the AEP Mountaineer Project. Greenh. Gas Sci. Technol. 2014;4:331-56.
[7] Manceau, JC, Rohmer, J. Post-injection trapping of mobile CO_2 in deep aquifers: Assessing the importance of model and parameter uncertainties. Comput. Geosci. 2016;20:1251-67.
[8] Mito, S, Xue, Z. Availability of a simplified coarse grid model for history matching at the Nagaoka post-injection CO_2 monitoring site. Energy Proc. 2017;114:5007-14.
[9] Lüth, S, Bergmann, P, Huang, F, Ivandic, M, Ivanova, A, Juhlin, C, Kempka, T. 4D seismic monitoring of CO_2 storage during injection and post-closure at the Ketzin pilot site. Energy Proc. 2017;July:5761-67.
[10] Dance, T, LaForce, T, Glubokovshikh, S, Ennis-King, J, Pevzner, R. Illuminating the geology: Post-injection reservoir characterization of the CO2CRC Otway site. Int. J. Greenh. Gas Control 2019;86:146-57.
[11] Chadwick, RA, Noy, DJ. Underground CO_2 storage: demonstrating regulatory conformance by convergence of history-matched modeled and observed CO_2 plume behavior using Sleipner time-lapse seismics. Greenhouse Gas Sci. & Tech. 2015;5:305-22.
[12] Harp, D, Onishi, T, Chu, S, Chen B, Pawar, RJ. Development of quantitative metrics of plume migration at geologic CO_2 storage sites. Greenhouse Gas Sci. & Tech. 2019;9(4):687-702.
[13] Pawar, RJ, Bromhal, G, Chu, S, Dilmore, RM, Oldenburg, C, Stauffer, P, Zhang, Y, Gurthrie, G. The National Risk Assessment Partnership's Integrated Assessment Model for Carbon Storage: A Tool to Support Decision Making Amidst Uncertainty. Int. J. Greenh. Gas Control 2016;52:175–89.
[14] Jiao, Z, Pawar, R, Duguid, A, Bouncier, W, Haussmann, C, Coddington, K, Harp, D, Ganshin, Y, Quillinan, S, McLaughlin, F, Ramsey, R. A field demonstration of an active reservoir pressure management through fluid injection and displaced fluid extraction at the Rock Springs Uplift A priority geologic CO_2 storage site for Wyoming. Energy Proc. 2017;114:2799-2811.
[15] Deng, H, Stauffer, PH, Dai, Z, Jiao, Z, Surdam, RS. Simulation of Industrial-Scale CO_2 Storage: Multi-Scale Heterogeneity and its Impacts on Storage Capacity, Injectivity and Leakage. Int. J. Greenh. Gas Control 2012;10, 397–418.
[16] Birkholzer, JT, Nicot, JP, Oldenburg, CM, Zhou, Q, Kraemer, S, Bandilla, K. Brine flow up a well caused by pressure perturbation from geologic carbon sequestration: Static and dynamic evaluations. Int. J. Greenh. Gas Control 2011;5:850-61.
[17] Birkholzer, JT, Cihan, A, Bandila, K. A tiered area-of-review framework for geologic carbon sequestration. Greenhouse Gas Sci. & Tech. 2014;4:20-35.
[18] Surdam, RC. Geological CO_2 Storage Characterization, first ed. New York: Springers; 2013.
[19] Carey, JW, Wigand, M, Chipera, SJ, WoldeGabriel, G, Pawar, R, Lichtner, PC, Wehner, SC, Raines, MA, Guthrie, GD. Analysis and performance of oil well cement with 30 years of CO_2 exposure from SACROC unit west Texas, USA. Int. J. Greenh. Gas Control 2007;1(1):75–85.
[20] Crow, W, Carey, JW, Gasda, S, Williams, DB, Celia, M. Wellbore integrity analysis of a natural CO_2 producer. Int. J. Greenh. Gas Control 2010;4:186–97.
[21] Gasda, S, Wang, JE, Celia, M. Analysis of in-situ wellbore integrity data for existing wells with long-term exposure to CO_2. Energy Proc. 2011;4:5406–13.